Available online at www.sciencedirect.com
ScienceDirect

Thermochimica Acta 462 (2007) 70–75

thermochimica acta

www.elsevier.com/locate/tca

Thermal conductivity of graphite/silicone rubber prepared by solution intercalation

Qiuhong Mu, Shengyu Feng [*]

Department of Chemistry and Chemical Engineering, Shandong University, Jinan 250100, PR China

Received 3 April 2007; received in revised form 20 June 2007; accepted 24 June 2007
Available online 29 June 2007

Abstract

Silicone/expanded graphite (EG) composites were prepared by melt mixing and solution intercalation. The effect of EG content and preparation methods of composites on thermal conductivity of composites were investigated, and it was found that with increasing EG, the thermal conductivity increased, and solution intercalation method showed better effect than melt mixing method in improving the thermal conductivity of composites. Dynamic mechanical analysis (DMA) was used to reveal that the storage modulus (E') of SI-prepared composite is relatively greater than those of MM-prepared composite counterparts. The scanning electron microscopes (SEM) observation confirmed that striking increase of thermal conductivity might be attributable to higher surface-to-volume ratio of EG fillers.

Keywords: Silicone rubber; Thermal conductivity; Nanocomposites; Morphology

1. Introduction

Since1987 the nylon 6/layered silicate nanocomposites were first prepared by intercalation polymerization in, the research and applications of layered silicate nanocomposites have made greatly progress. Layered silicates such as montmorillonite can be homogeneously dispersed in a polymer matrix in nanosheets to improve the desirable properties of the matrix and even generate new properties that cannot be derived from conventional composite counterparts. Layered silicates usually have very high aspect ratios (width-to-thickness). Once uniformly dispersed in a polymer matrix, properties of the polymer can be largely improved and some of them may not be shared by conventional composite counterparts [1–4].

Graphite is a layered mineral composed of weakly bonded graphene sheets with a large aspect ratio. It consists of a large number of graphene sheets held together by van der Waals forces. Single crystal graphite is one of the stiffest materials in nature with an elastic modulus of over 1 TPa, which is many times greater than nanoclay. Unlike clay, graphite is thermally and electrically conductive. It also has a lower density than clay. Expandable graphite, which is composed of natural graphite flake intercalated with acid, can be expanded up to hundreds of times over its initial volume at high temperature, resulting in separation of the graphene sheets at the nanoscopic level along the *c* axis of graphene layers [5–7]. During the last several years, a number of papers have studied on material preparation and characterization of various polymer nanocomposite systems reinforced with expanded graphite (EG) [8–12].

Natural graphite has excellent electrical and thermal conductivities. However, when it is mixed with polymers to make composites, its properties are generally reduced greatly [8]. To find a new method of preparing composites while keeping these properties as excellent as possible is always an interesting project in material science.

In view of the successful preparation of layered silicate nanocomposites by solution or melt intercalation, we attempted in this study to prepare silicone/EG thermal conducting nanocomposites by solution intercalation, in contrast to the conducting composites prepared by normal melt mixing.

2. Experimental

2.1. Materials

Methylvinylsilicone gum (M_n 5.8×10^5; mole content of vinyl group, 0.15%), silica and 2,5-bis(*tert*-butyl peroxy)-

---

[*] Corresponding author.
E-mail address: fsy@sdu.edu.cn (S. Feng).

0040-6031/$ – see front matter © 2007 Elsevier B.V. All rights reserved.
doi:10.1016/j.tca.2007.06.006

2,5-dimethyl hexane(DBPMH) were supplied by Chenguang Institute of Chemical Industry (Chengdu, China), Cabot China Ltd. (Shanghai, China) and Tianjin Akzo Nobel Peroxides Co. Ltd. (Tianjin, China), respectively. The graphite used in this study was expandable graphite with an average diameter of 300 μm and an expanded volume of 250 mL/g, supplied from Shandong Pingdu Jiaodong Graphite Co. (Qingdao, China).

2.2. *Sample preparation*

The expandable graphite was placed in an oven at 950 °C for rapid expansion and exfoliation to obtain the expanded graphite (EG).

2.2.1. *Melt mixing (MM) method*

Methylvinylsilicone gum, silica, EG and some other additives were rolled on a twin-roller at room temperature for certain time, followed by compression molding at 190 °C and 9.8 MPa for 20 min to obtain 120 mm × 40 mm plates with a thickness of 2 mm.

2.2.2. *Solution intercalation (SI) method*

The EG was dispersed in toluene to prepare a suspending dispersion with certain EG content. The methylvinylsilicone gum was dissolved in toluene by heating to a backflow temperature of toluene (about 100 °C). The EG suspending dispersion was added drop by drop into the methylvinylsilicone gum solution at the backflow state. After a backflow of 2 h, on cessation of heating, a portion of toluene was extracted under vacuum during the cooling process. Then resultant mixture was dried under vacuum. The resulting gum composites were pressed under the same conditions to obtain plates as in the MM method.

2.3. *Characterization*

Thermal conductivities of silicone rubber were tested with a thermally conductive probe instrument RTC-C (Fig. 1) (Ronghua Electronic Instrument Manufacture Co. Ltd., Jiangsu, China) by the stable state method, which was fabricated according to the ASTM D-5470. The size of specimen is 13.0 cm in diameter and 0.20 cm in thickness. Measurements were carried out by heating the heater blocks up to 100 °C, with the thermal pads clamped in between the two calorimeters in order to produce an average specimen temperature of 50 °C. For this, a chiller plate with circulating water at a temperature of 26 °C was placed above the cooling calorimeter to create a thermal gradient from the heating calorimeter to the cooling calorimeter. During measurements, an onset pressure of 1 bar was applied to reduce the effects of contact resistance between the specimen and the calorimeters due to minor surface irregularities. Readings from the thermocouples are recorded when equilibrium is achieved, whereby two successive set of temperature readings are taken at 15 min interval, shows a difference of ±0.1 °C. The thermal conductivity of the thermal pads were calculated from the Fourier's law, as is shown in Eq. (1), based on the assumption that the heat flow is one-dimensional in the perpendicular direction, and no heat loss occurs in the lateral direction:

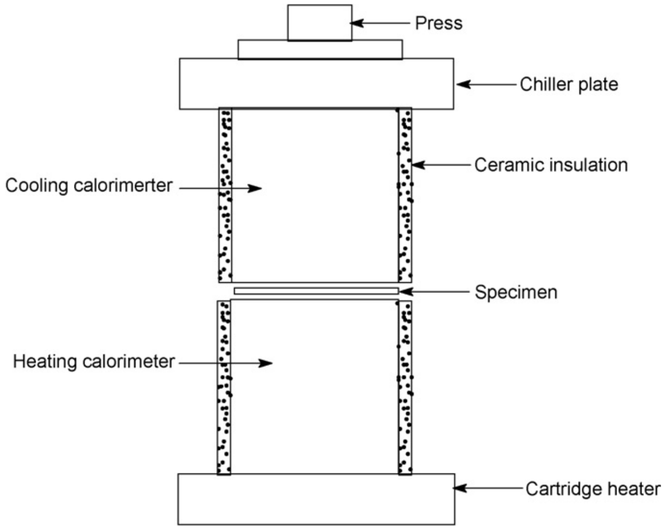

Fig. 1. Schematic diagram of thermally conductive probe instrument.

$$K = \frac{Qh}{A(T_{\text{hot\_int}} - T_{\text{cold\_int}})} \tag{1}$$

where K is the thermal conductivity of thermal pads ($\mathrm{W\,m^{-1}\,K^{-1}}$), the average heat flux (Q) is the amount of heat generated by two cartridge heaters, $T_{\text{hot\_int}}$ the interface temperature of the heating calorimeter (K), $T_{\text{cold\_int}}$ the interface temperature of the cooling calorimeter (K), A the surface area of tested thermal pads ($\mathrm{m^2}$), and h is the thickness of thermal pads (m).

The average heat flux (Q) is the amount of heat generated by cartridge heaters, while the interface temperature for both the heating and cooling calorimeter were extrapolated from the temperature gradients obtained from the thermocouples embedded in each of the calorimeter block. The thicknesses of the thermal pads (h) were measured using a digital camera, with pin guides embedded in the calorimeter blocks as guidelines.

The storage modulus of the samples was measured in the vertical mode using a dynamic mechanical analyzer (DMA 242, NETZSCH Instruments) at a fixed frequency of 1 Hz. The sample dimensions were 20 mm × 8 mm × 2 mm. The sample was tested with a temperature ranging from −130 °C up to room temperature at atmospheric pressure and a heating rate of 3 °C/min.

Morphological observations on the thermal conductive silicone rubber were done using the field emission scanning electron microscope (FE-SEM), JEOL JSM-7600F. In order to study the filler distribution and morphology, observations were carried out on the tensile broken surface of EG filled thermal conductive silicone rubber.

3. Results and discussion

3.1. *Thermal conductivity*

Fig. 2 represents the variation of the thermal conductivity of silicone/EG composites, prepared by the MM and SI methods,

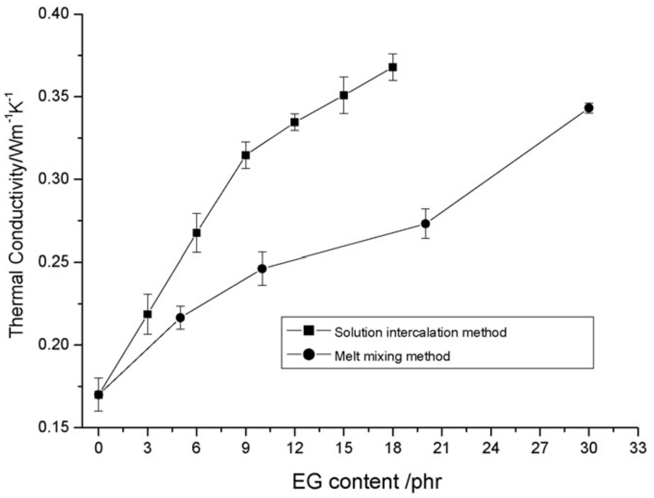

Fig. 2. Thermal conductivity vs. fraction of expanded graphite for silicone/EG composites prepared by two methods at 50 °C.

as a function of filler content. With the increase of EG content the thermal conductivity of silicone/EG composites were improved greatly. It was clearly that SI-prepared composite showed higher thermal conductivity than MM-prepared composite with the same filler content. The thermal conductivity of SI-prepared silicone/EG is $0.32\,\mathrm{W\,m^{-1}\,K^{-1}}$ at 9 per hundred rubbers (phr), whereas the MM-prepared composite was only $0.24\,\mathrm{W\,m^{-1}\,K^{-1}}$, which is the conductivity level similar to SI-prepared composite at 4 phr.

3.2. Dynamic mechanical properties

Fig. 3 shows the sample of the storage modulus E' for silicone/EG composites at 10 phr EG content as a function of temperature. It can be found that the log E' values of SI-prepared composite are relatively greater than those of MM-prepared composite counterparts, that is, the reinforcement effect for the SI-prepared composite is more dramatic than that for the MM-prepared composite. The results also demonstrate that the intercalation may restrict the flexibility of silicone molecular chains as well as increase the stiffness of the composite, resulting in the enhancement of the storage modulus. It is understood that the good dispersion of EG in silicone matrix could enhance the surface-to-volume ratio of EG and interfacial factors, which could on the whole contribute to potent stiffening effect for the composites.

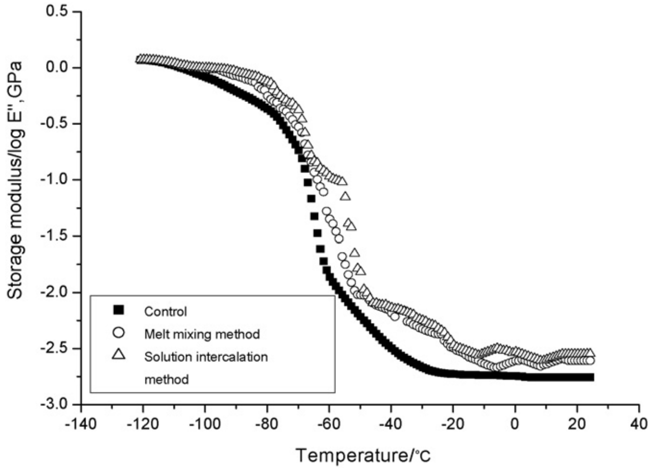

Fig. 3. Plots of storage modulus at 10 phr EG content as a function of temperature for samples.

It has been reported that there exists a correlation between the conductive network formation and the stiffening effect arising from the EG dispersion in the polymer solution [13]. From the above analysis, it is clear SI-prepared silicone/EG composites exhibits superior mechanical integrity in comparison with MM-prepared silicone/EG composites. It can be understand that the conductive network will reach faster for SI-prepared composites than for MM-prepared composites at same EG content, which is accordance with the results of Fig. 2.

3.3. Morphology and internal microstructure

The expandable graphite used was a kind of graphite intercalation compound (GIC), fabricated from natural flaky graphite (NFG) through chemical oxidation in the presence of concentrated sulfuric acid and nitric acid. The NFG is composed of layered, but compactly fastened nanosheets of graphite (Fig. 4(a)). The GIC differs from the NFG and is itself a nanocomposite, containing intercalating agents and characterized by increased interplanar spacing. The EG obtained by rapid heating of the GIC had much greater interplanar spacing than that of GIC, and thus emerged in a loose and porous vermicular shape. Its structure is basically parallel boards and sheets, which deform and collapse in an irregular pattern and then form a network-like structure with many pores of varied sizes, ranging from nanoscale to microscale (Fig. 4(b)–(d)). Fig. 4b reveals the loose structures of expanded graphite whereas Fig. 4(c) and (d) displays the photomicrographs of the loose structures in successively larger magnifications. Evidently, loose structures containing multi-pores in the EG could be observed in Fig. 4(c). For the EG prepared by the chemical method, the average pore diameter is about 2 mm. The surface area per gram is roughly 30–40 $\mathrm{m^2/g}$ and the pore volume is about 4–8 mL/g [14,15]. Fig. 4(d) also suggests the thickness of the EG layer is less than 100 nm. Thus, the galleries between the nanosheets of EG and pores in the EG network provide a larger space and can be easily intercalated by suitable monomers, catalysts, and even macromolecules.

Fig. 5 shows the SEM photographs of silicone/EG (10 phr) composites prepared by the two methods. It can be seen by comparison of Fig. 5(a) with Fig. 4(b)–(d) that the internal structure of EG in the composites prepared by the SI method was roughly identical to that of the original EG (i.e., they both emerged in a network structure), but the pore size and the board thickness in the former were larger and thinner than those in the latter. This suggests that, EG becomes solid after intercalating and can basically maintain its original network structure during compression molding. It can be observed from

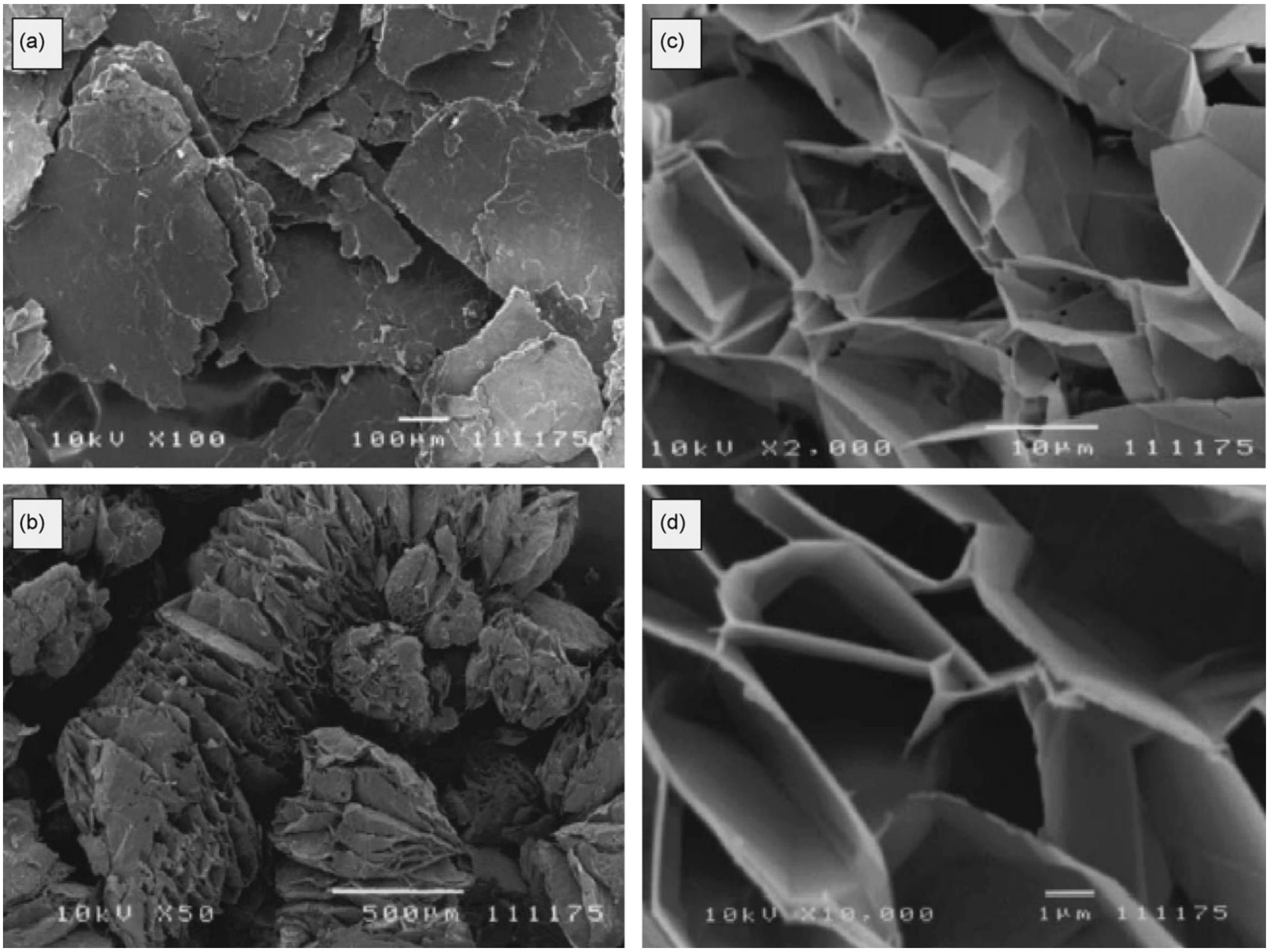

Fig. 4. SEM photomicrographs of (a) natural flake graphite, (b) expanded graphite (EG), (c) EG at higher magnification, and (d) abundant multipores with an interlayer thickness less than 100 nm are revealed in EG [13].

Fig. 5(b) that the original long vermicular EG was fragmented, and most of the multi-pores in EG had been filled by the silicone molecules. At the interfacial regions, good contacts exist between the matrix polymer and the EG filler, indicating strong polymer–filler interactions. Moreover, because the intercalation of silicone can promote the exfoliation of graphite boards and sheets as well as enlarge the space between them, the EG/silicone network formed had a larger size and finer structure (Fig. 5(c)) than those of the original EG network, characterized by a greater aspect ratio of the sheets and boards. However, pronounced changes in the internal structure of EG took place in the composite prepared by the MM method (Fig. 5(d)). The boards and sheets of graphite were severely bent and bundled and both the interplanar space and the pore sizes obviously diminished. This means that the original EG network was largely destroyed under stress because of the absence of silicone.

The SEM observations mentioned earlier revealed the differences in the morphology and internal microstructure of the silicone/EG composites prepared by two methods from different structure levels. It can be concluded that the nanocomposites prepared by solution intercalation had multiple network structure, which was composed of the particles, the boards or sheets, and the nanosheets with different scales. On the contrary, there were no such multiple networks existing in the normal composites prepared by melt mixing. This can be attributed to the fact that during solution intercalation, the silicone molecules can more sufficiently intercalate the pores and galleries of EG through the solvation effect of toluene, the physical absorption of EG pores, driven by the solution flow at the boiling state and the extraction under vacuum. Moreover, as the intercalation process proceeded, the graphite boards and sheets might be further delaminated and exfoliated, which would allow more silicone molecules to intercalate and enlarge the space between them. Thus, the intercalated silicone can support, improve, and solidify the formed EG/silicone network, thus preventing the network from destruction under stress. Compared with the case mentioned above, the silicone molecules that entangled each other in the highly viscous melt cannot intercalate the spacing between the sheets of EG under shear stress or compression; at most, they can infiltrate only the larger pores of EG. Consequently, the original EG network was destroyed to a large extent under the stress, which have been proved by Fig. 5(d).

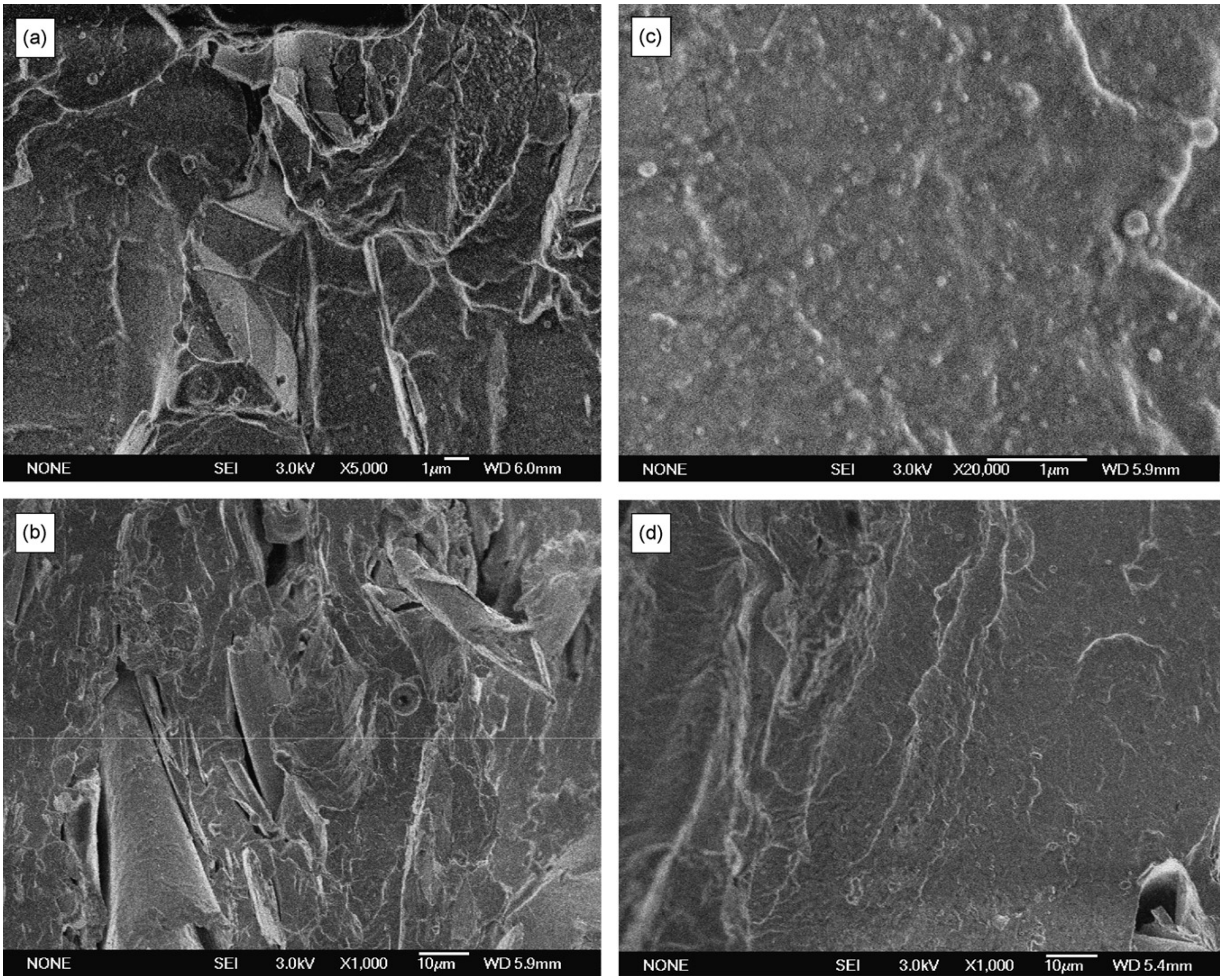

Fig. 5. SEM micrographs of silicone/EG (10 phr) composites prepared by solution intercalation (a–c) and melt mixing (d).

3.4. Formation of thermal conducting paths

The electrically conducting mechanism of polymer composites is associated with one key question: how to form the conducting paths [16]? Since the thermal conduction system has some analogy with the electric conduction system, it can be found that the formation of the thermal conductive paths is great of importance. In previous studies, it has been proved that the more conductive particles the more conductive paths can be formed. But if we can obtain more thermal conductive parts with the same particles content, i.e., get higher thermal conductivity with lower volume content of filler, the contradiction between high thermal conductivity and good processing behavior can be solved in certain degree. In fact, the dispersed morphology of thermal conducting fillers in polymer matrices greatly depends on geometrical factor of filler. Hence, the formation mechanism of thermal conducting paths is related to the fact that the conducting filler particles with different morphologies and internal microstructures can form the paths by distinct ways or patterns. For the silicone/EG conducting composites investigated in this study, according to their thermal conductivity—filler content relations as shown in Fig. 2, EG with different morphologies and internal microstructures can be introduced to focus on the formation mechanism of conducting paths. The models illustrated in Fig. 6 can be used to interpret it.

For the nanocomposites prepared by solution intercalation (Fig. 6(a)), the EG particles with a large surface-to-volume ratio can abut or contact and then form a conducting path network at lower EG contents, resulting from the intercalation of silicone into them and thus forming EG/silicone nanoscale and microscale networks, which protect the EG particles from destruction during compression. Therefore, low addition of filler showed higher thermal conductivity. As to the normal composites prepared by melt mixing (Fig. 6(b)), the EG particles' shape is drastically changed during the melting processing, resulting in the reduction of the surface-to-volume ratio. Consequently, only at higher EG contents can they abut or contact and form the conducting paths.

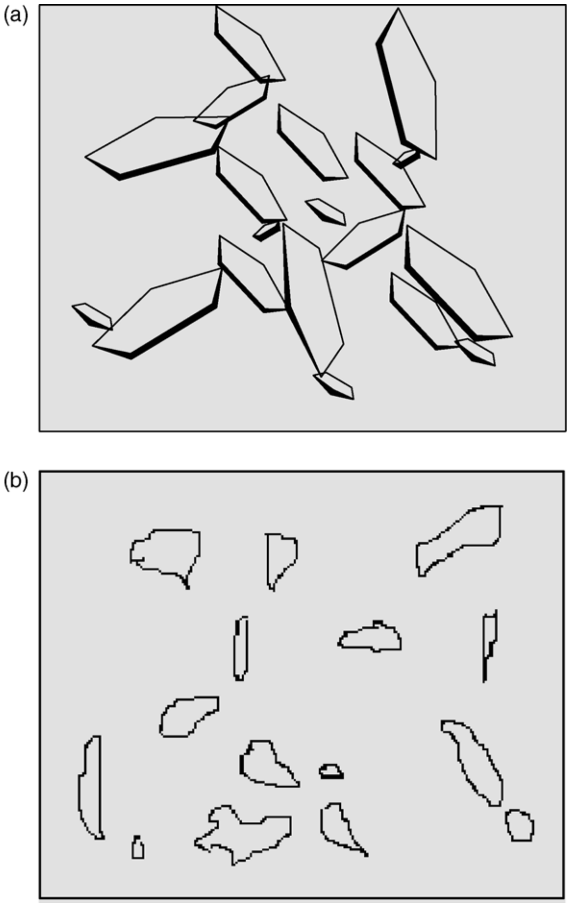

Fig. 6. Structural models of silicone/EG composites prepared by (a) solution intercalation and (b) melt mixing, showing the formation of conducting paths.

4. Conclusions

Solution intercalation was used to prepare the silicone/EG thermally conductive composites. In contrast with the conventional composites prepared by melt mixing, the thermal conductivity of the composites was much higher. When the EG content was 9 phr, the thermal conductivity of the former reaches $0.32\,\mathrm{W\,m^{-1}\,K^{-1}}$, whereas the latter was only $0.24\,\mathrm{W\,m^{-1}\,K^{-1}}$. DMA results demonstrate that the intercalation may restrict the flexibility of silicone molecular chains as well as increase the stiffness of SI-prepared composite, resulting in the enhancement of the storage modulus. As observed from SEM micrographs, EG fillers dispersed in silicone matrix showed different surface-to-volume ratio. For SI-prepared composites, the EG particles with a large surface-to-volume ratio can abut or contact and then form a conducting path network at lower EG contents. It can be concluded that the surface-to-volume ratio of EG fillers played a deciding role in the striking improvement of thermal conductivity of the composites.

Acknowledgements

The financial support by Foundation for University Key Teacher, Ministry of Education and Reward Funds for the Outstanding Young, Shandong University are gratefully acknowledged.

References

[1] M. Alexandre, P. Dubois, Polymer-layered silicate nanocomposites: preparation, properties and uses of a new class of materials, Mater. Sci. Eng. 28 (2000) 1–59.
[2] S.C. Jana, S. Jain, Dispersion of nanofillers in high performance polymers using reactive solvents as processing aids, Polymer 42 (2001) 6897–6905.
[3] C. Saujanya, S. Radhakrishnan, Structure development and crystallization behaviour of PP/nanoparticulate composite, Polymer 42 (2001) 6723–6731.
[4] W.-P. Wang, C.-Y. Pan, Preparation and characterization of polystyrene/graphite composite prepared by cationic grafting polymerization, Polymer 45 (2004) 3987–3995.
[5] W.-G. Zheng, S.-C. Wong, H.J. Sue, Transport behavior of PMMA/expanded graphite nanocomposites, Polymer 43 (2002) 6767–6773.
[6] G.-H. Chen, D.-J. Wu, W.-G. Weng, W.-L. Yan, Preparation of polymer/graphite conducting nanocomposite by intercalation polymerization, J. Appl. Polym. Sci. 82 (2001) 2506–2513.
[7] G.-H. Chen, D.-J. Wu, W.-G. Weng, B. He, W.-L. Yan, Preparation of polystyrene–graphite conducting nanocomposites via intercalation polymerization, Polym. Int. 50 (2001) 980–985.
[8] Y.-X. Pan, Z.-Z. Yu, Y.-C. Ou, G.-H. Hu, New process of fabricating electrically conducting nylon 6/graphite nanocomposites via intercalation polymerization, J. Polym. Sci. B: Polym. Phys. 38 (2000) 1626–1633.
[9] J.-W. Shen, W.-Y. Huang, S.-W. Zuo, J. Hou, Polyethylene/graphite nanocomposites: preparation, structure, and electrical properties, J. Appl. Polym. Sci. 97 (2005) 51–59.
[10] W.-P. Wang, Y. Liu, X.-X. Li, Ye-Z. You, Synthesis and characteristics of poly(methyl methacrylate)/expanded graphite nanocomposites, J. Appl. Polym. Sci. 100 (2006) 1427–1431.
[11] A. Celzard, M. Krzesinska, D. Begin, J.F. Mareche, S. Puricelli, G. Furdin, Preparation, electrical and elastic properties of new anisotropic expanded graphite-based composites, Carbon 40 (2002) 557–566.
[12] D. Cho, S. Lee, G. Yang, H. Fukushima, L.T. Drzal, Dynamic mechanical and thermal properties of phenylethynyl-terminated polyimide composites reinforced with expanded graphite nanoplatelets, Macromol. Mater. Eng. 290 (2005) 179–187.
[13] W.-G. Zheng, S.-C. Wong, Electrical conductivity and dielectric properties of PMMA/expanded graphite composites, Compos. Sci. Technol. 63 (2003) 225–235.
[14] J.-P. Liu, K.-M. Song, Study on the preparation of expandable graphite, J. Funct. Mater. 29 (1998) 659–661 (Chinese).
[15] N. Cao, W. Shen, S. Wen, Y. Liu, Surface properties of expanded graphite, Chem. Bull. 4 (1996) 37–42.
[16] J.-W. Shen, X.-M. Chen, W.-Y. Huang, Structure and electrical properties of grafted polypropylene/graphite nanocomposites prepared by solution intercalation, J. Appl. Polym. Sci. 88 (2003) 1864–1869.